Biomaterials 30 (2009) 3996–4005

Contents lists available at ScienceDirect

Biomaterials

journal homepage: www.elsevier.com/locate/biomaterials

In-vitro osteogenesis of synovium stem cells induced by controlled release of bisphosphate additives from microspherical mesoporous silica composite

Xuetao Shi [a,b,1], Yingjun Wang [a,c,*,1], Rohan R. Varshney [b], Li Ren [a,c], Feng Zhang [b], Dong-An Wang [b,c,**]

[a] School of Materials Science and Engineering, South China University of Technology, Guangzhou 510641, China
[b] Division of Bioengineering, School of Chemical and Biomedical Engineering, Nanyang Technological University, Singapore 637457, Republic of Singapore
[c] Key Laboratory of Specially Functional Materials and Advanced Manufacturing Technology, South China University of Technology, Ministry of Education, Guangzhou 510641, China

ARTICLE INFO

Article history:
Received 21 January 2009
Accepted 19 April 2009
Available online 13 May 2009

Keywords:
Mesoporous silica
Synovium-derived mesenchymal stem cell
Alendronate
Osteogenesis
Controlled release
Bisphosphate

ABSTRACT

In this study, in-vitro osteogenesis was successfully induced in the highly chondrogenic synovium mesenchymal stem cells (SMSCs) by controlled release of a nitrogenous bisphosphonate additive – alendronate (AL) from a mesoporous silica (MS)–hydroxyapatite (HA) composite that was mediated in poly(lactic-co-glycolic acid) (PLGA) microspheres. This microspherical based controlled release system is constructed with three levels of degradable structures: (1) the AL drug was first hybridized with HA nanoparticles; (2) the HA–AL complexes were filled into the mesopores of MS particles by self-assembly *in situ*; and (3) the HA–AL-laden MS constructs (MSH–AL) were built in the bulk of PLGA microspheres. In comparison with any mono-component construct, the superiority of this multi-component system comes from two aspects of functionalities: (1) significantly greater loading capacity of the extremely hydrophilic drug-AL; and (2) better controlled profile of AL release. Based on this newly developed PLGA/MSH–AL releasing system, as recipients the SMSCs, which usually exhibit exclusively high chondrogenesis, demonstrated a strong osteogenic commitment. The results were verified by alkaline phosphatase (ALP) activity assay, calcium secretion assay, real time PCR and immunohistochemistry analysis. Considering the renewable source and high proliferative profile of SMSCs, the achievement of engineered SMSC osteogenesis with this PLGA/MSH–AL controlled release system would open a new door to major bony reparation and regeneration.

1. Introduction

Synovium-derived mesenchymal stem cells (SMSCs), first identified and isolated in 2001, are a new member in MSC families [1]. Compared with MSCs derived from bone marrow (BMSCs), SMSCs have higher colony-forming efficiency, growth kinetics, and fold increase [2]. Additionally, synovial tissue has high self-regenerative capability and can fully heal after harvesting a part of the tissue by synovectomy; therefore, as a source of therapeutic cells, it possesses the valuable advantages of both abundance and renewal [3]. Although generally MSCs belong to a multipotent category of progenitors and are capable of differentiating into various cell types like chondrocytes, osteoblasts, adipocytes and myocytes, yet, SMSCs specifically show a dominant tendency to differentiate into chondrocytic species instead of osteoblastic progenies [4]. To date, there are few reports mentioning osteogenesis of SMSCs and especially null for their engineering use towards bony formation. Owing to the excellent proliferative and regenerative properties of SMSCs, if we could manage the engineered osteogenesis with them, it would be a great contribution to bone-related regenerative medicine.

Alendronate (AL) is a nitrogenous bisphosphonate (BP) consisting of stable analogues of natural pyrophosphate compounds that inhibit bone resorption by osteoclasts. It is widely used in the clinical treatment of systemic metabolic bone diseases such as Paget's disease, osteoporosis, hypercalcemia of malignancy, as well as inflammation-related bone loss [5–7]. Besides inhibiting osteoclast viability, AL is also found to promote osteoblast proliferation and maturation and can even facilitate the osteoblastic differentiation of human BMSCs [8,9]. In this study, we attempt AL as a functional additive to enable SMSCs' osteogenesis and make it suitable for engineered use.

In order to achieve efficient osteogenesis of SMSCs by AL treatment, a superior controlled release system for optimal AL loading

* Corresponding author. School of Materials Science and Engineering, South China University of Technology, Guangzhou 510641, China.
** Corresponding author. Division of Bioengineering, School of Chemical and Biomedical Engineering, Nanyang Technological University, 70 Nanyang Drive, N1.3-B2-13, Singapore 637457, Republic of Singapore. Tel.: +65 6316 8890; fax: +65 6791 1761.
E-mail addresses: imwangyj@scut.edu.cn (Y. Wang), dawang@ntu.edu.sg (D.-A. Wang).
[1] These authors contributed equally to this manuscript.

0142-9612/$ – see front matter © 2009 Elsevier Ltd. All rights reserved.
doi:10.1016/j.biomaterials.2009.04.021

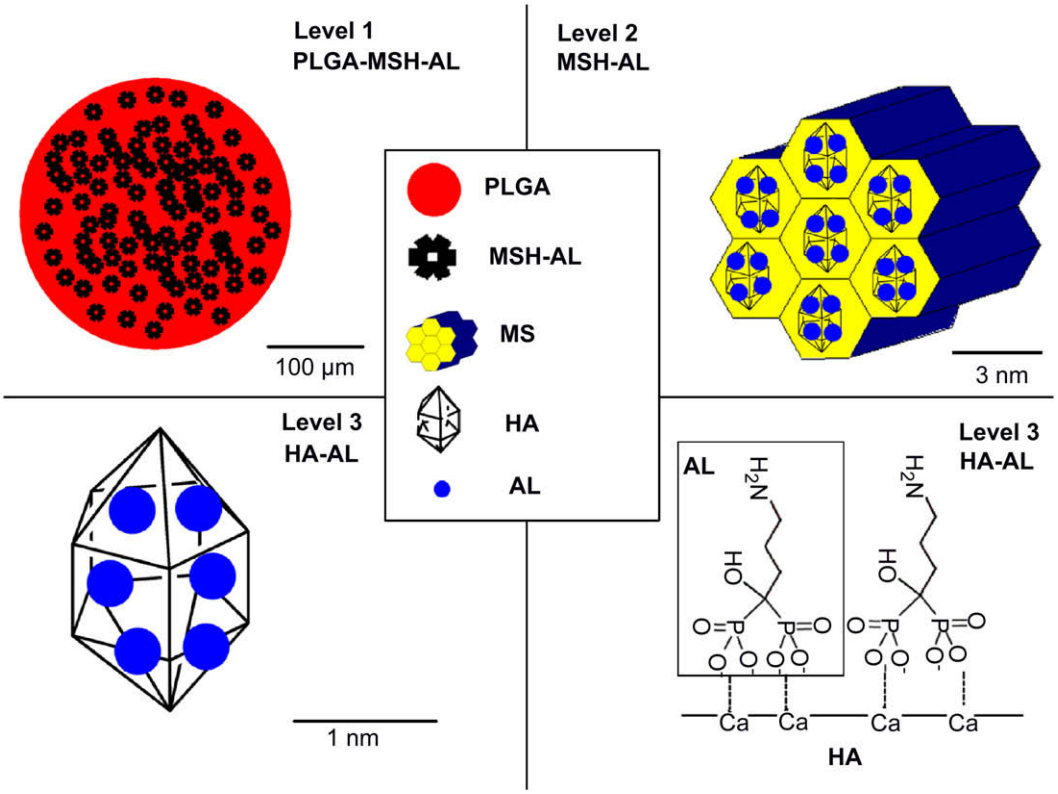

Fig. 1. The scheme of PLGA/MSH–AL's three-level structure. This microspherical based controlled release system is constructed with three levels of degradable structures: (Level 3) the AL drug was first hybridized with HA nanoparticles; (Level 2) the HA–AL complexes were filled into the mesopores of MS particles by self-assembly *in situ*; and (Level 1) the HA–AL-laden MS constructs (MSH–AL) were built in the bulk of PLGA microspheres.

and delivery is in imperative demand. To fulfill an ideally controlled release of AL that is highly hydrophilic and therefore very easily lost in aqueous conditions during processing or application, the optional carriers must be able to ensure the retention of AL loading and simultaneously to avoid side effects such as the cytotoxicity of high AL dosage. The candidate materials could be poly(lactic-co-glycolic acid) (PLGA) microspheres, chitosan, hydroxyapatite (HA) or mesoporous silica (MS) and so on [10–12]. Among them, HA has the highest AL loading efficiency as AL molecules are capable of strongly binding to calcium phosphate crystals so as to adjustably counteract the tendency of AL loss during aqueous treatments [13,14]. Besides the improvement in loading efficiency, our previous study found that, being hybridized with HA, the desired AL release could also be sustained longer (over one month). In this study, in pursuit of an even better matrix for controlled release of AL, we further explored an innovative composite system based on HA and MS [15].

The utilization of MS for drug controlled delivery was first proposed in the year 2001 [16]. MS particles possess a highly regular nano-porous structure with uniform pore size and a vast surface area, which makes them very useful for the manner of controlled release as well as an excellent protection for the loaded guest molecules [17–22]. In this work, the adopted MS-co-HA composite (MSH) was fabricated via self-assembling methods proposed by Andersson et al. [23]. In this way, the material not only inherits the high surface area produced by nano-pores on MS but also possesses the beneficial biocompatibility of both HA and the silica [24].

The entire AL releasing system is finalized by packaging the AL-laden MSH constructs into PLGA microspheres – in whole

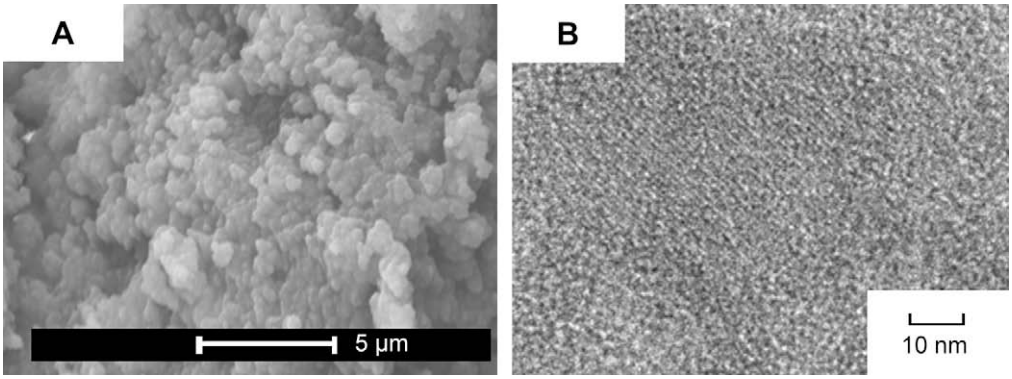

Fig. 2. SEM (A) and HRTEM (B) images of MSH.

Table 1
Real time RT-PCR primer sets.

Gene	Direction	Sequence (5′–3′)
Osteocalcin	Forward	GAAGCCCAGCGGTGCA
	Reverse	CACTACCTCGCTGCCCTCC
BMP-2	Forward	CGCCTCAAATCCAGCTGTAAG
	Reverse	GGGCCACAATCCAGTCGTT
Collagen I	Forward	ATCAAGGAAGGGCAAACGAG
	Reverse	GGCAACAGCAGGTTCACTTACA
Runx-2/Cbfa-1	Forward	TGATGACACTGCCACCTCTGA
	Reverse	GCACCTGCCTGGCTCTTCT
GAPDH	Forward	TCGTCCTCCTCTGGTGCTCT
	Reverse	CCACTTTGTGAAGCTCATTTCCT

abbreviated as "PLGA/MSH–AL" system (Fig. 1), based on which, an engineered osteogenesis of SMSCs is manipulated and investigated.

2. Materials and methods

2.1. Materials

Tetraethyl orthosilicate (TEOS), ethyl alcohol (EtOH), $Ca(NO_3)_2$ and $(NH_4)_2HPO_4$ were purchased from Chemical Reagent Factory (Guangzhou, China). Dodecylamine (DDA) was supplied by SSS Reagent Co., Ltd (Shanghai, China). PLGA (lactic/glycolic 1:1; M_w 31,000 Da; inherent viscosity 0.30 dL/g in chloroform at 30 °C) was purchased from Daigang Biomaterials Inc. (Jinan, China). Alendronate (AL) was purchased from Tianfeng Inc. (Henan, China). Poly(vinyl alcohol) (PVA), β-glycerophosphate, ascorbic acid and dexamethasone were obtained from Sigma–Aldrich (Singapore). All cell-culture related reagents were purchased from Gibco (Invitrogen, Singapore).

2.2. Synthesis methods

2.2.1. MSH particles

The synthesis of MSH was carried out via the method described in reference [22]. Briefly, DDA was used as a template, it was dissolved in an EtOH/deionized water solution containing $Ca(NO_3)_2$, $(NH_4)_2HPO_4$ and NH_4OH at a pH = 9. TEOS was used as a silica source. The reaction mixture conformed to the following molar composition: TEOS: 1.0, DDA: 0.27, EtOH: 9.09, H_2O: 29.6, $Ca(NO_3)_2$: 1.0, $(NH_4)_2HPO_4$: 0.6. The mixture was stirred for 1 h and then aged for another 18 h at ambient temperature. The product was dried in an oven at 90 °C. The template of the product was removed via hot EtOH extraction at 75 °C and sintering at 500 °C.

2.2.2. MSH–AL particles

MSH–AL particles were prepared by adding 5 g plain MSH particles (Fig. 2) into 100 ml AL solution (0.5 mg/ml). The solution was kept at 37 °C under constant stirring for 24 h. The deposited phase was isolated and washed in deionized water for three times and then dried. The MSH–AL particles so obtained were sieved to select particles smaller than 50 μm diameter for further use.

2.2.3. PLGA/MSH–AL microspheres

PLGA/MSH–AL microspheres were manufactured by dissolving 3 g PLGA into 30 ml methylene chloride in which MSH–AL particles (2.4 g and 3.6 g) were added. The mixture emulsion was stirred for 3 h, and then poured into 1000 ml 1% PVA aqueous solution and stirred at 300 rpm for 4 h. The resultant PLGA/MSH–AL microspheres were isolated, then washed in deionized water and dried in air for 24 h. And PLGA/MSH was fabricated by the same method.

2.3. Morphological characterization

Morphological characterization was conducted using scanning electron microscopy (SEM, 30XLFEG, Philips, The Netherlands). PLGA/MSH–AL microspheres or MSH particles were immobilized on a cupreous stub and coated with gold. MSH particles were dispersed in ethanol and their morphology was characterized by HRTEM (JEM-2010, JEOL, Japan) using an accelerating voltage of 200 kV.

2.4. Microsphere size analysis

A light-scattering particle size analyzer (Matersizer 2000, Malvern Instrument Ltd, British) was used to determine the size distribution of the prepared microspheres. The lyophilized particles (2 g) were suspended in a large amount of distilled water (800 ml) and analyzed under continuous stirring.

2.5. Determination of HA amount assembled into MS

One hundred milligrams of MSH particles were immersed into acetic acid aqueous solution (pH = 3.5) for 4 h. After 4 h, the samples were collected and then dried, the dry weight of the sample (M) was determined. HA amount assembling into MSH was determined as $(100 - M)$ mg.

2.6. Determination of AL encapsulation efficiency

(i) *MSH–AL particles*. The AL encapsulation efficiency of MSH–AL particles was determined by suspending 50 mg MSH–AL into 2 ml PBS buffer (pH = 7.2) and incubating at 37 °C during which the supernatant was periodically analyzed following the method reported in reference [25].

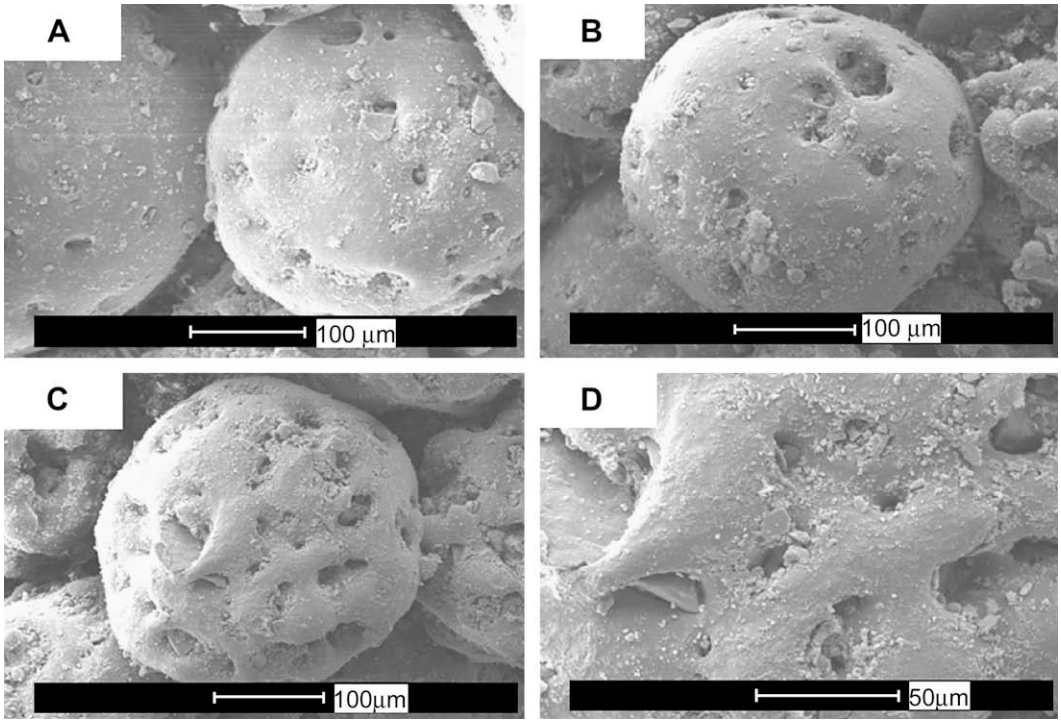

Fig. 3. SEM images of PLGA/MSH–AL. (A and B) PLGA/MSH–AL with 80% MSH–AL; (C and D) PLGA/MSH–AL with 120% MSH–AL.

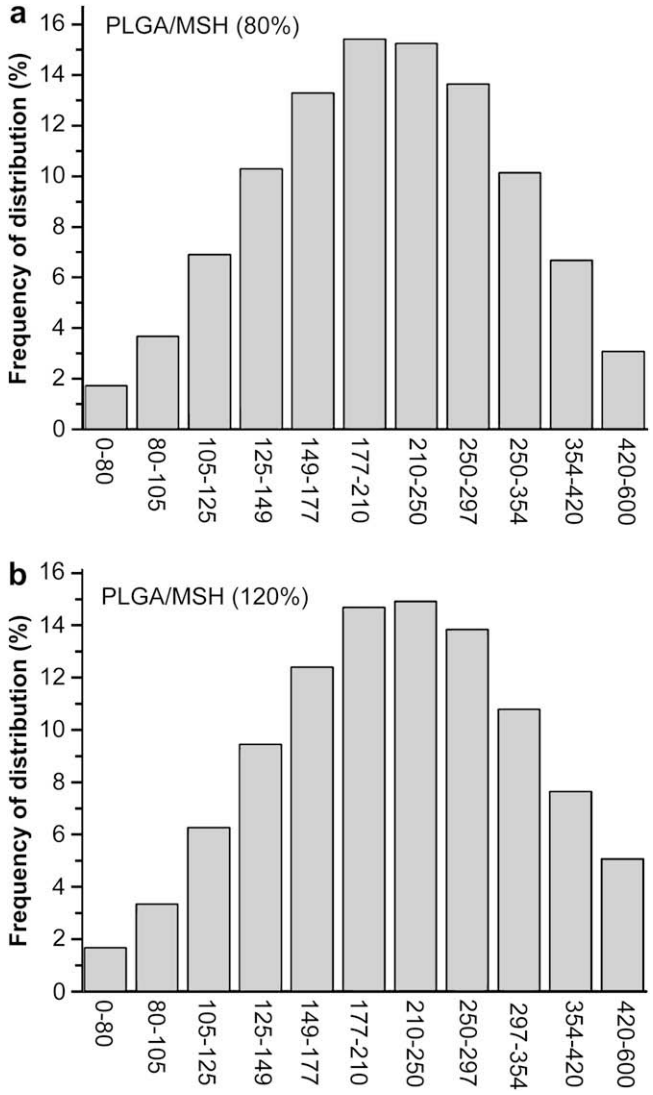

Fig. 4. Diameter distribution of PLGA/MSH–AL with 80% and 120% MSH–AL content.

(ii) *PLGA/MSH–AL microspheres.* PLGA/MSH–AL microspheres (0.2 g) were suspended in methylene chloride (30 ml) to deposit the insoluble MSH–AL particles out. The deposited MSH–AL particles and all supernatants were collected respectively. The portion of encapsulated AL in MSH–AL particles (C_{MSH-AL}) was measured as described above. The collected supernatant, which is an AL suspension in PLGA methylene chloride solution, was rinsed in iron(III) chloride/perchloric acid solution to extract the suspended AL into the aqueous phase. The AL in the iron(III) chloride/perchloric acid solution extraction, which represents the AL encapsulated in PLGA matrix (C_{PLGA}), was quantified using UV spectrophotometer following the method described in reference [25,26]. The total AL loading amount in PLGA/MSH–AL microspheres was calculated as ($C_{MSH-AL} + C_{PLGA}$) and was used to determine the encapsulation efficiency. Therefore, the total AL encapsulation efficiency in PLGA/MSH–AL microspheres could be calculated by ($C_{MSH-AL} + C_{PLGA}$)/C_{TID}, in which C_{TID} represents the total initial dosage of AL devoted for the whole process.

2.7. In-vitro release of AL from PLGA/MSH–AL microspheres

In-vitro AL release trials were performed in a shaking incubator at 60 rpm under 37 °C. Fifty milligrams of AL-loaded microspheres were soaked in 200 ml PBS (pH = 7.2). Sample media were collected at regular time intervals with equal amount of PBS makeup.

2.8. Cell culture

Six-week-old New Zealand white rabbit (weight: 1.49 kg) was purchased from The National University of Singapore (Singapore). Rabbit synovium-derived mesenchymal stem cells (MSCs) were harvested using the method described in reference [27] and were propagated in Dulbecco's modified Eagle's medium (DMEM) supplemented with 1.5 mg/ml sodium bicarbonate, 4.5 mg/ml glucose, 10% (v/v) fetal bovine serum (FBS), 100 units/ml penicillin, and 100 μg/ml streptomycin. The passage 3 SMSCs were used in this study.

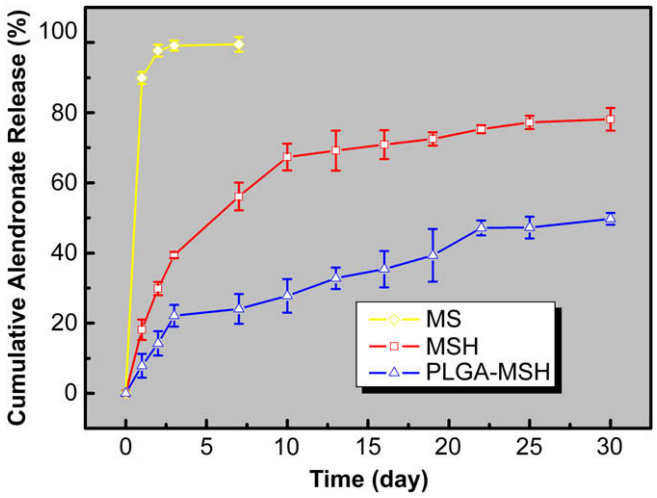

Fig. 5. Cumulative release of AL from MS, MSH particles and PLGA/MSH–AL.

2.9. Cytotoxicity assay

Cytotoxicity was evaluated with MTT [3-(4,5-dimethylthiazol-2-yl)-2,5-diphenyltetrazolium bromide, Roche Diagnostics, Germany] assay. Briefly, PLGA/MSH–AL microspheres (50 mg) and MSH–AL (22 mg) were placed in 24-well TCPS (tissue culture polystyrene) plates and cells (1×10^4 cells/ml) were seeded in the same wells and altogether incubated in a humid atmosphere under 37 °C and 5% CO_2 for various periods of time before conducting the MTT assay following the standard protocol. Cells seeded on bare TCPS (no involvement of microspheres) in the cultural media were used as control.

2.10. Cell seeding and proliferation on PLGA/MSH–AL

PLGA/MSH–AL was pre-wetted in the culture medium for 12 h. Fifty microlitres of the cell suspension (1×10^6 cells/well) were seeded into the pre-wetted microspheres (100 mg). The microspheres were left in the humidified incubator for 2 h to allow cells to attach on them, and then 750 μl of culture medium was added to each scaffold. The microspheres with cells were cultured at 37 °C in a humidified incubator with 5% CO_2 for 14 days. Cell proliferation was assessed using a Live/Dead assay kit (Invitrogen, Singapore) following the manufacturer's instruction. Cell attachment and proliferation were determined using Hoechst assay (Hoechst 33258, Molecular Probes, Invitrogen), following the manufacturers' instructions. Via the measured

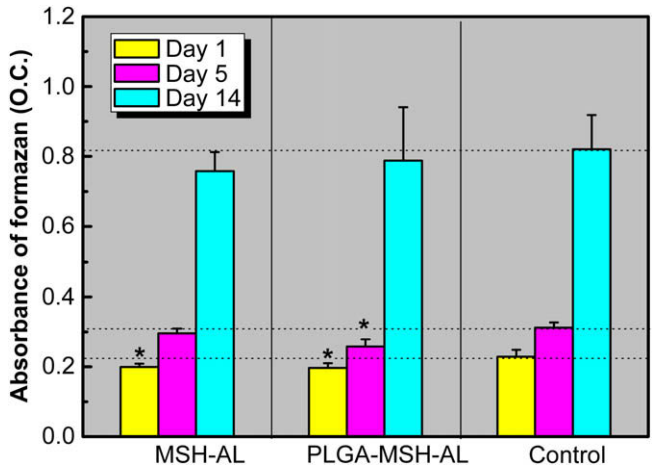

Fig. 6. Cytotoxicity of MSH–AL particles and PLGA/MSH–AL. * indicates statistical significance when compared with control ($p < 0.05$).

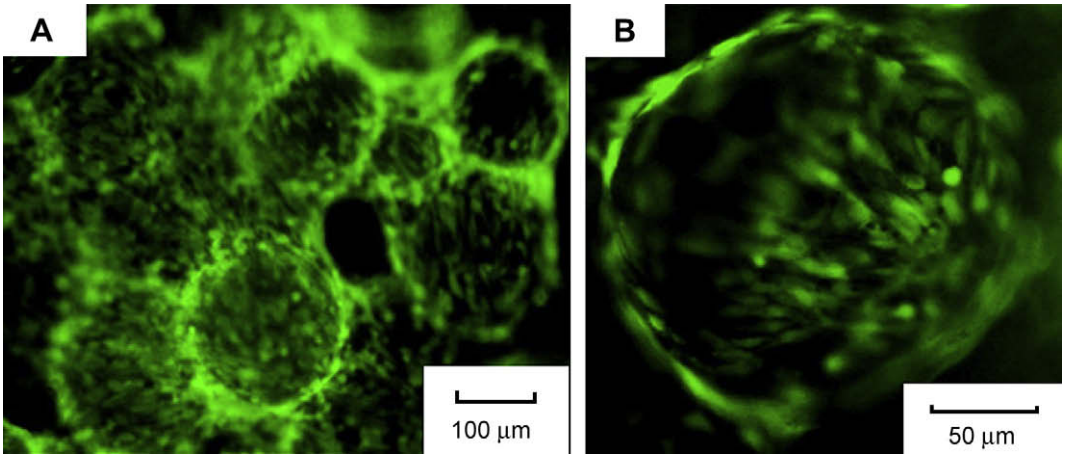

Fig. 7. Fluorescence photographs of SMSC proliferation on PLGA/MSH–AL scaffolds after 14 days.

DNA quantities, the exact numbers of the committed cells could be counted using a conversion rate of 6.6 pg DNA per cell.

2.11. Monolayer culture

After expansion to three passages, SMSCs were trypsinized and replated onto 24 well TCPS (tissue culture polystyrene) plates with a density of 1×10^4 cells/ml/well and incubated in a humid atmosphere under 37 °C and 5% CO_2. Cells were allowed to adhere and to grow for 3 days. Following this period, the medium was replaced with osteogenic medium [DMEM supplemented with 10% FBS, 100 nM dexamethasone, 50 mg/ml ascorbic acid, and 10 mM β-glycerophosphate; OGM] containing soluble AL released from PLGA/MSH–AL microspheres. In the control groups, cells were cultured on PLGA/MSH in OGM, DMEM supplemented with 10% FBS, and on PLGA/MSH–AL in combination with DMEM with 10% FBS, respectively. The media were changed every 3 days. Osteogenesis was assessed by alizarin red staining at Day 14 after the initial osteogenic induction.

2.12. Three-dimensional culture

Osteogenic differentiation was induced by incubating cell laden scaffolds (PLGA/MSH and PLGA/MSH–AL) in OGM for 21 days. Alkaline phosphatase (ALP) activity was determined using *p*NPP assay (*p*-nitrophenyl phosphate liquid substrate, Sigma Diagnostics). Briefly, MSCs that had been pre-washed with PBS were lysed in 0.5 ml PBS containing 0.1 M glycine, 1 mM $MgCl_2$ and 0.05% Triton X-100. The lysate was incubated with *p*-nitrophenyl phosphate (*p*NPP) solution at 37 °C for 30 min, and then subjected to a spectrophotometer on which the absorbance at 405 nm was measured and recorded to indicate ALP concentration. The alizarin red-based assay of mineralization was performed according to reference [28]. The ALP and mineralization outcomes were further normalized against the cell numbers.

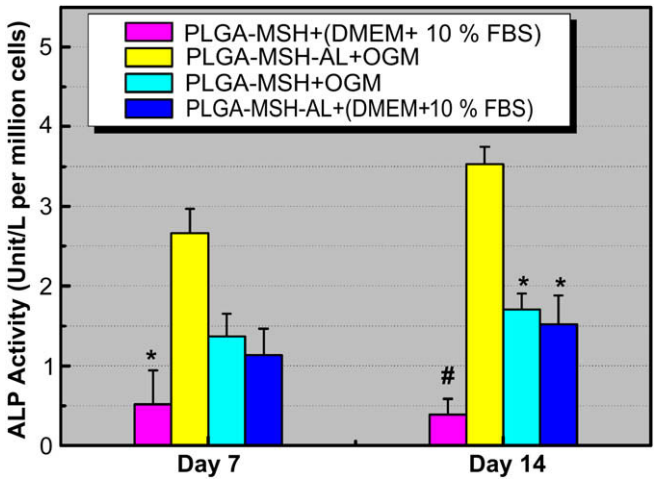

Fig. 8. Alkaline phosphate activity in SMSCs cultured on PLGA/MSH and PLGA/MSH–AL in DMEM + 10% FBS and OGM. * indicates statistical significance when compared with PLGA/MSH–AL + OGM ($p < 0.05$), and # indicates statistical significance when compared with PLGA/MSH + OGM, PLGA/MSH–AL + OGM and PLGA/MSH–AL + DMEM + 10% FBS ($p < 0.05$).

2.13. Real time quantitative reverse transcription-polymerase chain reaction

Real time quantitative reverse transcription-polymerase chain reaction (real time RT-PCR) was performed as follows: total RNA was isolated from cells which underwent osteogenic differentiation for 21 days following TRIzol protocol and subjected to RT with SuperScript™ First-Strand Synthesis System (Promega, USA). The complementary DNA (cDNA) yield was then subjected to PCR to examine the gene expression of osteocalcin (OC), type I collagen, BMP-2, Runx-2/Cbfa-1, and β-actin. The adopted primer sequences and PCR conditions are listed in Table 1. Quantitative polymerase chain reaction (qPCR) was conducted using SYBR green assay (iQ supremix, Bio-rad, USA). The gene expressions were quantified by calculating $2^{-\Delta C_T}$ values, where C_T represents the cycle number when an arbitrarily placed threshold was reached, and $\Delta C_T = (C_{T,\text{target gene}} - C_{T,\beta\text{-actin}})$. Cells cultured on PLGA/MSH in DMEM + 10% FBS was used as control.

2.14. Immunohistochemistry

Immunohistochemistry assay was conducted as follows: after 21 days culture, cell laden three-dimensional microspheres were fixed in 4% paraformaldehyde solution for 30 min. Thereafter the fixed specimens were incubated in 10% goat blocking serum for 1 h to suppress non-specific binding of IgG. The specimens were then incubated in the collagen I primary antibody (2 ng/mL, mouse monoclonal IgG, Santa Cruz Biotechnology, USA) or osteocalcin primary antibody (2 ng/mL, rabbit polyclonal IgG) at 37 °C for 1 h and Anti-IgG (5 ng/mL, Invitrogen Alexa Fluor, 488) or Anti-IgG (5 ng/mL, Invitrogen Alexa Fluor, 546) at room temperature for 1 h followed by 3 washes in PBS. The specimens were then observed under fluorescent microscope (Olympus, IX71, Japan).

2.15. Statistical analysis

Six completely independent experiments (six separate microsphere samples) were performed for every assay and the results were expressed as means ± standard deviations. Statistical significance was calculated using one way analysis of variance (one-way ANOVA). Comparison between the two means was performed using Tukey test and data was determined as statistically significant for $p < 0.05$.

3. Results

3.1. Morphology and characteristics of MSH

The morphology and structure of MSH were investigated by SEM (Fig. 2). MSH particles maintained an irregular sheet-shaped surface morphology and their sizes were between 300 nm and 600 nm. From HRTEM image of MSH [Fig. 2(B)], the continuous parallelism of the lattice fringes with the same orientation as that of HA crystals suggests oriented apatite assembly and formation of a regular structure into MS particles [24]. The surface area and median pore diameter of MSH were 332 m^2/g and 3.3 nm

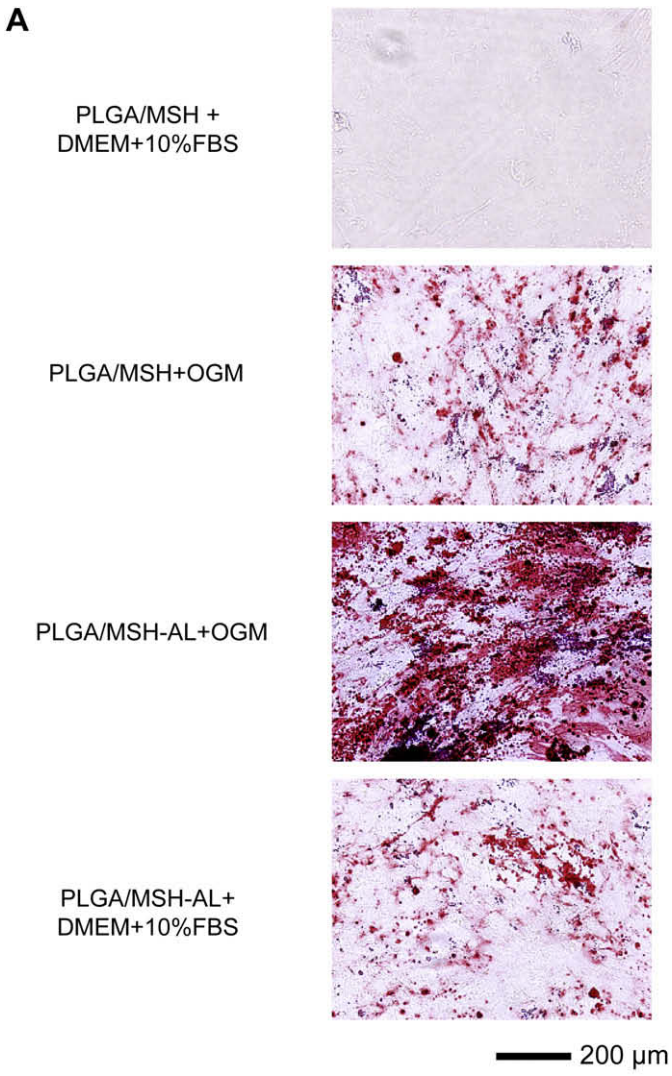

Fig. 9. Mineralization and calcium secretion by SMSCs cultured on PLGA/MSH–AL and PLGA/MSH–AL in DMEM + 10% FBS and OGM using alizarin staining (A) and semi-quantificational alizarin red-based assays (B), respectively. * and & indicate statistical significance when compared with PLGA/MSH–AL + OGM and PLGA/MSH–AL + DMEM + 10% FBS ($p < 0.05$), and # indicates statistical significance when compared with PLGA/MSH + OGM, PLGA/MSH–AL + OGM and PLGA/MSH–AL + DMEM + 10% FBS ($p < 0.05$).

respectively, which are smaller and larger than those of MS respectively because of the assembly and growth of HA into MS [24]. The HA content in MSH was 44.2 ± 5.6%.

3.2. Morphology and characteristics of PLGA/MSH–AL

PLGA/MSH–AL was fabricated in such a way that AL molecules were loaded onto HA and HA–AL self-assembled into mesoporous silica *in situ* and these were then all together filled into PLGA matrix (Fig. 1). The morphology of PLGA/MSH–AL is shown in Fig. 3. The drug-laden microsphere maintains a spherical shape and also presents a wrinkling morphology due to greater MSH–AL enrichment. It is also observable that a lot of pores are distributed on the surface of PLGA/MSH–AL and this porous morphology is more distinct for PLGA/MSH(120%)–AL–SM. The phenomenon may be attributed to the shedding of MSH–AL particles from PLGA microspheres during the fabrication process.

Data of microspherical size distribution for both types of microspheres (PLGA/MSH (120%)–AL, PLGA/MSH(80%)–AL) are listed in Fig. 4. PLGA/MSH (120%) AL are slightly larger sized than microspheres with 80% MSH–AL particle content. The average sizes of PLGA/MSH (80%)–AL and PLGA/MSH (120%)–AL were 245 μm and 258 μm respectively. A large number of MSH–AL particles were shed from PLGA/MSH (120%)–AL matrix during the fabrication of the composite microspheres, therefore composite microspheres with 80% MSH–AL content were chosen as AL carriers.

3.3. In-vitro drug delivery

The AL release profile of MSH is shown in Fig. 5. The release profile exhibits an exponential tendency and the burst release of AL from MSH for the first four days is more than 40% of total AL loading amount. MS was also used as an AL carrier, but the AL release profile of MS presents an extremely significant initial burst, in which almost 90% of total AL loading amount was released within the first day. It is evident that MSH particles are more favorable vehicles for AL release than MS.

The profile of AL (cumulative in vitro) release over 30 days from PLGA/MSH–AL is also shown in Fig. 5. The curve is comparable to the release curve of MSH–AL despite a minimal bursting initiation. According to the trend, 20–30% of total AL loading amount was released from PLGA/MSH–AL during the first four days. However, compared with MSH, PLGA/MSH–AL presents a significantly slower release. It can also be observed that the AL release curve takes on a visible ascending tendency. On Day 30, the total AL release from MSH and PLGA/MSH–AL had reached around 80% and 50%, respectively.

3.4. Cytotoxicity evaluation

Cell toxicity of MSH–AL, PLGA/MSH–AL and PLGA/MSH was analyzed using MTT assay after 1, 5 and 14 days of culture. The MTT assay analyzes the viability of cells by measuring the activity of the mitochondrial dehydrogenases. As shown in Fig. 6, an increase in absorbance from Day 1 to Day 14 was recorded, which indicates a trend of increasing cell proliferation for all the groups. Cell viability on PLGA/MSH–AL and MSH–AL was comparable to the control group. In addition, hydroxyapatite and PLGA were also confirmed to have minimal cytotoxicity [29,30]. Taken together, the results demonstrate that PLGA/MSH–AL and MSH–AL particles have minimal cytotoxicity. SMSC adhesion on PLGA/MSH–AL was demonstrated via live/dead assay staining and DNA quantification kit (Fig. 7). Around 53% seeded cells were attached on PLGA/MSH–AL microsphere after 24 h of culture. After 14 days culture on the microspheres, cells grew well

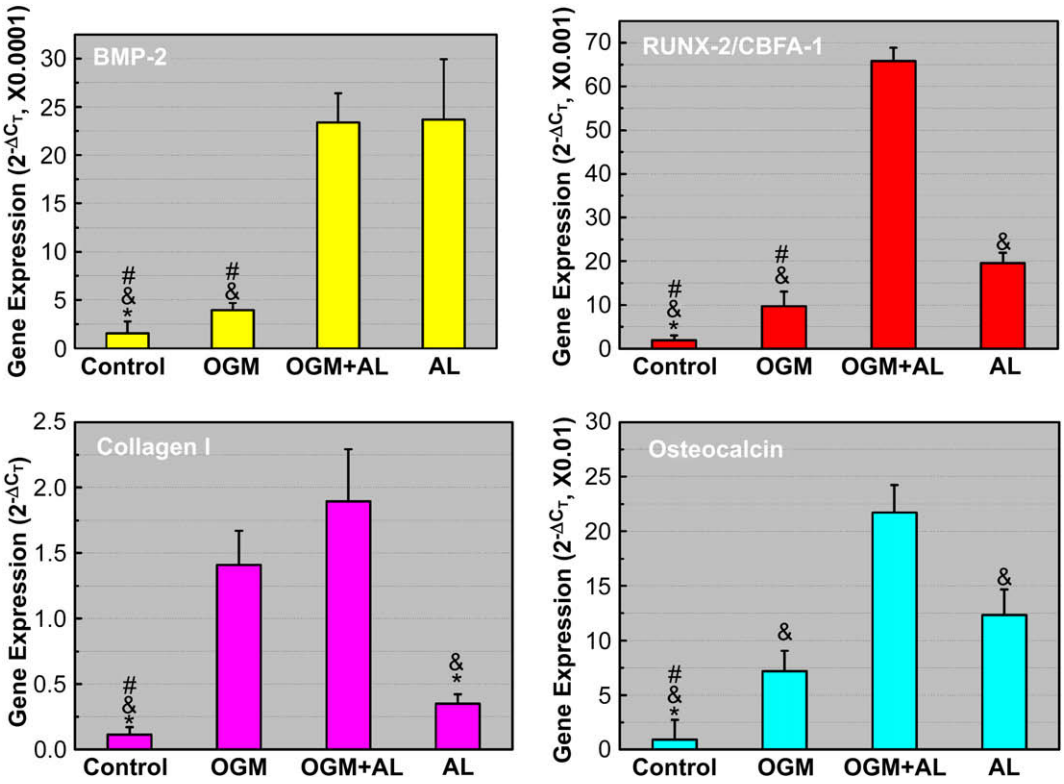

Fig. 10. Gene expression of osteocalcin, BMP-2, Runx-2/Cbfa-1, and collagen I using real-time PCR. #, & and * indicate statistical significance when compared with PLGA/MSH–AL + DMEM + 10% FBS, PLGA/MSH–AL + OGM, and PLGA/MSH + OGM ($p < 0.05$).

and proliferated on the microspherical surface and cell growth-induced microspherical conglutination was observed.

3.5. Osteogenesis

In this study, SMSCs on the scaffolds were made to undergo osteogenic differentiation. The secretion of ALP, a standard marker of osteogenic differentiation, was determined by *p*NPP assay (Fig. 8). Positive ALP production was detected at Day 7, followed by significant upregulation on Day 14. SMSCs treated by AL released from PLGA/MSH–AL in osteogenic media displayed significantly higher levels of ALP secretion compared to those only treated by OGM.

A critical important function of osteogenic cells is participating in biological mineralization. Calcium deposition by osteogenic cells was assessed by alizarin staining at Day 14 [Fig. 9(A)] and semi-quantificational alizarin red-based assays at Day 7 and Day 14 [Fig. 9(B)]. After 7 and 14 days of culture, a significantly higher level of calcium secretion was observed from cells cultured with AL released from PLGA/MSH–AL in OGM. Contrastively, there was no remarkable calcium secretion in SMSCs cultured in DMEM with 10% FBS after 14 days culture.

Gene expression of bone-relevant markers in SMSCs was determined by real-time RT-PCR at Day 21. Cells on PLGA/MSH–AL cultured in OGM had significantly higher expression of the well acknowledged early and late bone markers – Runx-2/Cbfa-1 and OC, and other bone relevant markers – type I collagen and BMP-2, as shown in Fig. 10. The expression of BMP-2 in cells cultured on PLGA/MSH–AL in DMEM + 10% FBS is comparable to that in cells cultured on PLGA/MSH–AL in OGM.

Immunohistochemistry staining of cellular aggregates (for type I collagen and OC) cultured on PLGA/MSH–AL and PLGA/MSH in OGM and DMEM + 10% FBS is shown in Fig. 11. After 21 days of culture, type I collagen and OC secreted from SMSCs cultured on PLGA/MSH–AL in OGM display significantly intensive fluorescence. However, there is only weak fluorescence staining of cells on PLGA/MSH–AL in DMEM + 10% FBS and PLGA/MSH in OGM, indicating weak osteogenic capacity of SMSCs cultured in OGM only and in AL containing DMEM + 10% FBS. The analysis of collagen I and OC expression was conducted by observing the whole sections of surface fluorescence under fluorescent microscope (Olympus, IX71, Japan).

4. Discussion

SMSCs can be easily harvested from synovial membrane tissue and the harvest process has low invasiveness and causes minimal complications at the donor site. Compared with bone marrow derived mesenchymal stem cells (BMSCs), which are widely used in bone regeneration, SMSCs have higher expansion ability. Besides, Sakaguchi et al. [1] reported that colony number of nucleated SMSCs (per 1000) was more than 100-fold higher than that of BMSCs. A high self-renewal capacity of SMSCs was also reported by De Bari et al. [31]. Their easy and safe harvesting procedure and high proliferation rate render SMSCs as particularly suited for engineered applications in tissue repair.

SMSCs have the highest chondrogenic potential among BMSCs, SMSCs and MSCs derived from periosteum, adipose and muscle tissues. However, SMSCs show remarkably weak osteogenic ability compared to BMSCs and there are few reports on the osteogenesis of SMSCs, especially in vitro. In this study, we found that after treatment with AL in combination with OGM, SMSCs exhibited significantly higher osteogenic commitment than when treated with OGM alone, with AL in combination with DMEM + 10% FBS or with DMEM + 10% FBS alone. von Konch et al. [9] reported that AL has

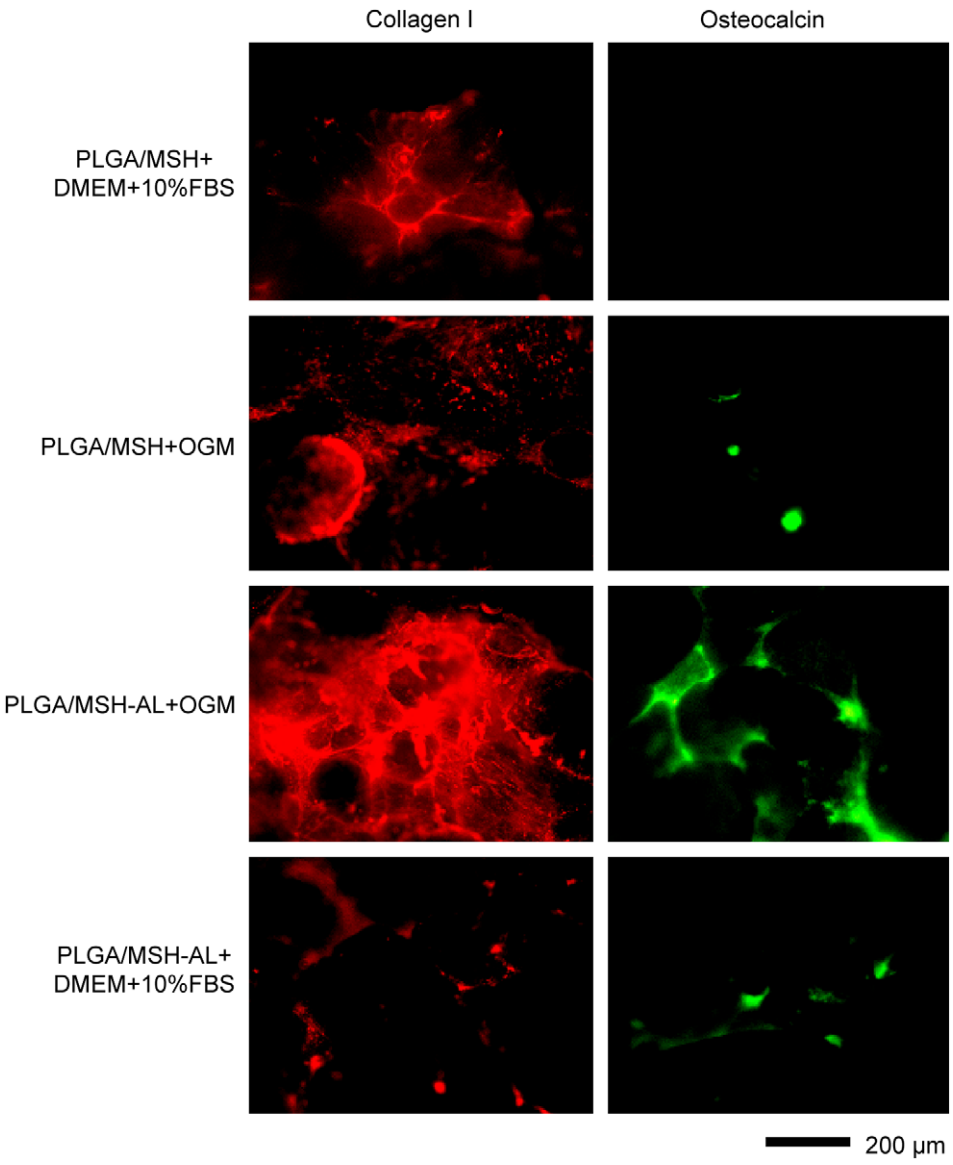

Fig. 11. Three-dimensional images for immunohistochemistry staining of type I collagen and osteocalcin secreted by SMSCs cultured on PLGA/MSH and PLGA/MSH–AL in DMEM + 10% FBS and OGM for 21 days respectively.

a positive effect on the osteogenic differentiation of BMSCs. However, we found that the osteogenic commitment of SMSCs treated by AL in combination with DMEM + 10% FBS is comparable to that of SMSCs treated with OGM alone, but is significantly weak compared with that of SMSCs treated with AL in combination with OGM.

ALP is expressed mainly on cell surfaces or in matrix vesicles. It specifically degrades the organic phosphoesters in bone and cartilage, which inhibits cartilage mineralization and promotes calcium deposition in bone [32]. Gene expression of ALP increases before mineralization, and subsequently decreases after the initiation of mineralization. OC is an important late bone marker that regulates the formation and growth of bone minerals and therefore indicates the finalization of osteogenesis [33]. Type I collagen constitutes an overwhelming majority (over 90%) of bony structural proteins and takes major responsibility for the tensile strength of the tissue and also provides templates for mineralization [34]. After being treated by AL in combination with OGM, SMSCs showed high ALP activity (Fig. 8) and high expression of OC and Type I collagen (Fig. 10). The cells cultured on the AL free microspheres in DMEM + 10% FBS exhibited super low OC expression (Fig. 10) and no visible OC secretion by immunohistochemistry assay (Fig. 11).

As shown in Fig. 10, we found remarkable Runx2/Cbfa-1 and BMP-2 expression in cells in AL containing groups. Runx2/Cbfa-1 is known to upregulate transcription of osteoblast marker genes such as those encoding OC, type I collagen and osteopontin (OPN) by binding to specific enhancer regions containing the core sequence [35]. Therefore, it plays an important role in the maintenance of the differentiated state of osteoblasts. BMP-2 is crucial for osteogenesis and bone formation and its expression is dramatically increased in primitive mesenchymal and chondrocytic cells during endochondral ossification [34]. AL acts by interfering with the mevalonate pathway of cholesterol synthesis by inhibiting farnesyl diphosphate synthase. This leads to reduction of geranylgeranyl diphosphate required for prenylation of guanosine triphosphate (GTP)-binding proteins, which are essential for osteoclast activity [35–40]. The inhibition of mevalonate pathway by BPs can stimulate osteoblasts by inducing expression of BMP-2 [41]. As can be seen in our results, cells treated with AL containing media had significantly higher

expression of BMP-2. The positive expression of osteogenic markers by SMSCs treated with AL and OGM indicates successful osteogenic induction and provides a foundation for developing a brand new osteogenic medium recipe based on AL, β-glycerophosphate, ascorbic acid and dexamethasone for SMSCs.

Because of its strong hydrophilicity, AL exhibits low encapsulation efficiency in traditional polymeric controlled release systems. The AL encapsulation efficiency of PLGA microsphere was only $7.10 \pm 1.55\%$ [15], and most of the free drug molecules lapsed during the fabrication process. In this work, AL was loaded onto HA which self-assembled into the pores of MS particles and the AL-laden MSH particles were further encapsulated in PLGA matrix. The three leveled structure facilitated much higher encapsulation efficiency – $77.56 \pm 8.52\%$ and slower controlled release of AL. PLGA–HA microsphere was also used as AL vehicle in our previous study [15]. Compared with PLGA and PLGA–HA microsphere based AL release system, PLGA/MSH–AL exhibited lower release rate and only 50% of the encapsulated AL was released by Day 30.

As shown in Fig. 1, this microspherical based controlled release system is constructed with three levels of degradable structures: (1) the AL drug was first hybridized with HA; (2) the HA–AL complexes were filled into the mesopores of MS particles by self-assembly *in situ*; and (3) the HA–AL-laden MS constructs (MSH–AL) were built in the bulk of PLGA microspheres. Therefore, the AL release for these three levels is multiple: (1) the release of AL from HA is controlled by the solubility of HA; (2) mesoporous silica is utilized as a vehicle of HA–AL, and at the same time, it also assumes an active role for enhancement of AL encapsulation and the retardation of AL release as reported by Nieto et al. [42]; (3) PLGA closed down the open mesopores of MSH–AL, which induced another switch for release of AL from the entire microspherical system. The AL release from PLGA is attributed to degradation of PLGA and diffusion of the drug out of microspheres.

Besides slowing down AL release from MSH particles, PLGA also takes on another active role. Hybridizing PLGA with MSH prevents MSH particles from being swept off from the implant by flowing body fluids. Furthermore, PLGA/MSH microspheres produced by single emulsion technique can also be categorized as a beneficial cell carrier. SMSC adhesion on PLGA/MSH–AL was demonstrated via live/dead assay staining (Fig. 7). After 14 days culture on the microspheres, cell growth-induced microspherical conglutination was observed, which was mainly due to over-confluence of cells on microspherical surfaces. The phenomenon has also been observed on other microcarriers such as chitosan coated PLGA microspheres and gellan microspheres [43,44]. Microspherical conglutination is beneficial for the constitution of new tissue with better continuity and integrity [45].

PLGA based microspheres have also been proven to be a good injectable scaffold for bone and cartilage regeneration applications [46]. Injectable scaffolds are useful in repairing defective tissue via minimally invasive surgical procedures [47–49]. Besides its potential use as an injectable scaffold, PLGA/MSH–AL can also be used to fabricate microsphere sintered scaffolds through the technique developed by Borden et al. [50].

5. Conclusion

In this study, osteogenic differentiation of SMSCs – which have a strong chondrogenic tendency – on AL-laden PLGA/MSH–AL was achieved successfully in OGM. AL loaded PLGA/MSH microspheres were fabricated by single emulsion technique. PLGA/MSH microspheres and MSH particles exhibited controlled release of AL without remarkable initial burst release and sustained release for more than a month. PLGA/MSH–AL and MSH–AL exhibited low cytotoxicity and PLGA/MSH–AL promoted SMSC proliferation on its surface. Strong osteogenic markers such as ALP, type I collagen, osteocalcin, Runx-2/Cbfa-1 and BMP-2 were dramatically expressed when SMSCs were cultured on PLGA/MSH–AL in OGM. To sum up, PLGA/MSH–AL hybrid microspheres being a promising injectable and multifunctional vehicle with wide ranging applications, this *in situ* AL delivery system could be utilized as a favorable carrier of AL for engineered osteogenesis.

Acknowledgements

Shi Xuetao is a China Scholarship Council (CSC) scholarship recipient (2007U33046). This research was supported by National Natural Science Foundation of China (Grant 50572029), the Key Programs of the Ministry of Education (Grant 305012), the State Key Program of National Natural Science of China (Grant 50732003). The research was also supported by Grant ARC 10/06, Ministry of Education, Singapore. The authors are grateful to Fan Jiabing (Sun Yat-Sen University, China) for his help with SMSC harvest and culture.

Appendix

Figures with essential colour discrimination. Certain figures in this article, in particular parts of Figures 1, 7, 9 and 11, are difficult to interpret in black and white. The full colour images can be found in the on-line version, at doi:10.1016/j.biomaterials.2009.04.021.

References

[1] Sakaguchi Y, Sekiya I, Yagishita K, Muneta T. Comparison of human stem cells derived from various mesenchymal tissue: superiority of synovium as a cell source. Arthritis Rheum 2005;52:2521–9.
[2] Djouad F, Bony C, Häupl T, Uzé G, Lahlou N, Louis-Plence P, et al. Transcriptional profiles discriminate bone marrow-derived and synovium-derived mesenchymal stem cells. Arthritis Res Ther 2005;7:1304–15.
[3] Koga H, Muneta T, Ju Y-J, Nagase T, Nimura A, Mochizuki T, et al. Synovial stem cells are regionally specified according to local microenvironment after implantation for cartilage regeneration. Stem Cells 2007;25:689–96.
[4] Fan JB, Varshney RR, Ren L, Cai DZ, Wang DA. Synovium-derived mesenchymal stem cells: a new cell source for musculoskeletal regeneration. Tissue Eng B 2009;15:75–86.
[5] Stresing V, Daubiné, Benzaid I, Mönkkönen H, Clézardin P. Bisphosphonates in cancer therapy. Cancer Lett 2007;257:16–35.
[6] Fisher JE, Rogers MJ, Halasy JM, Luckman SP, Hughes DE, Masarachia PJ, et al. Alendronate mechanism of action: geranylgeraniol, an intermediate in the mevalonate pathway, prevents inhibition of osteoclasts formation, bone resorption, and kinase activation in vitro. Proc Natl Acad Sci U S A 1999;96:133–9.
[7] Kavanagh KL, Guo K, Dunford JE, Wu X, Knapp S, Ebetino FH, et al. The molecular mechanism of nitrogen-containing bisphophonates as anti-osteoporosis drugs. Proc Natl Acad Sci U S A 2006;103:7829–34.
[8] Gun-Il I, Sheeraz AQ, Jennifer K, Harry ER, Arun SS. Osteoblast proliferation and maturation by bisphosphonates. Biomaterials 2004;25:4105–15.
[9] von Konch F, Jaquiery C, Kowalsky M, Schaeren S, Alabre C, Martin I, et al. Effects of bisphosphonates on proliferation and osteoblast differentiation of human bone marrow stromal cells. Biomaterials 2005;26:6941–9.
[10] Nafea EH, EI-Massik MA, EI-Khordagui LK, Marei MA, Khalafallah NM. Alendronate PLGA microspheres with high loading efficiency for dental applications. J Microencapsul 2007;24:525–38.
[11] Patashnik S, Rabinovich L, Golomb G. Preparation and evaluation of chitosan microspheres containing bisphosphonates. J Drug Target 1997;4:371–80.
[12] Balas F, Manzano M, Horcajada P, Vallet-Regi M. Confinement and controlled release of bisphosphonates on ordered mesoporous silica-based materials. J Am Chem Soc 2006;128:8116–7.
[13] Palazzo B, Iafisco M, Laforgia M, Margiotta N, Natile G, Bianchi CL, et al. Biomimetic hydroxyapatite–drug nanocrystals as potential bone substitutes with antitumor drug delivery properties. Adv Funct Mater 2007;17:2180–8.
[14] Boanini E, Gazzano M, Rubini K, Bigi A. Composite nanocrystals provide new insight on alendronate interaction with hydroxyapatite structure. Adv Mater 2007;19:2499–502.
[15] Shi X, Wang Y, Ren L, Gong Y, Wang D-A. Enhancing alendronate release from a novel PLGA/hydroxyapatite microspheric system for bone repairing applications. Pharm Res 2009;26:422–30.
[16] Vallet-Regí M, Balas F, Arcos D. Mesoporous materials for drug delivery. Angew Chem Int Ed 2007;46:7548–58.
[17] Slowing II, Trewyn BG, Giri S, Lin VSY. Mesoporous silica nanoparticles for drug delivery and biosensing applications. Adv Funct Mater 2007;17:1225–36.

[18] Charnay C, Bégu S, Tourné-Péteih C, Nicole L, Lerner DA, Devoisselle JM. Inclusion of ibuprofen in mesoporous templated silica: drug and release property. Eur J Pharm Biopharm 2004;57:533–40.
[19] Tozuka Y, Ogushi T, Yamamoto K. Adsorption and entrapment of salicylamide molecules into the mesoporous structure of folded sheets mesoporous material (FSM-16). Pharm Res 2003;20:926–30.
[20] Liong M, Lu J, Kovochich M, Xia T, Ruehm SG, Nel AE, et al. Multifunctional inorganic nanoparticles for imaging, targeting, and drug delivery. ACS Nano 2008;2:889–96.
[21] Torney F, Trewyn BG, Lin VSY, Wang K. Mesoporous silica nanoparticles deliver DNA and chemicals into plants. Nat Nanotechnol 2007;2:295–300.
[22] Luckarift HR, Spain JC, Naik RR, Stone MO. Enzyme immobilization in a biomimetic silica support. Nat Biotechnol 2004;22:211–3.
[23] Andersson J, Areva S, Spliethoff B, Lindén M. Sol–gel synthesis of a multifunctional, hierarchically porous silica/apatite composite. Biomaterials 2005;26:6827–35.
[24] Shi X, Wang Y, Wei K, Ren L, Lai C. Self-assembly of nanohydroxyapatite in mesoporous silica. J Mater Sci Mater Med 2008;19:2933–40.
[25] Shi X, Wang Y, Ren L, Zhao N, Gong Y, Wang D-A. Novel mesoporous silica based antibiotic releasing scaffold for bone repair. Acta Biomater, doi:10.1016/j.actbio.2009.01.010.
[26] Kuljanin J, Janković I, Nedeljković J, Prstojević D, Marinković V. Spectrophotometric determination of alendronate in pharmaceutical formulations via complex formation with Fe(III) ions. J Pharm Biomed 2002;28:1215–20.
[27] Yokoyama A, Sekiya I, Miyazaki K, Ichinose S, Hata Y, Muneta T. In vitro cartilage formation of composites of synovium-derived mesenchymal stem cells with collagen gel. Cell Tissue Res 2005;322:289–98.
[28] Gregory CA, Gunn WG, Peister A, Prockop DJ. An alizarin red-based assay of mineralization by adherent cells in culture: comparison with cetylpyridinium chloride extraction. Anal Biochem 2004;329:77–84.
[29] Hsu FY, Chueh S-C, Wang YJ. Microspheres of hydroxyapatite/reconstituted collagen as supports for osteoblast cell growth. Biomaterials 1999;20:1931–6.
[30] Jabbarzadeh E, Jiang T, Deng M, Nair LS, Khan YM, Laurencin CT. Human endothelial cell growth and phenotypic expression on three dimensional poly(lactide-co-glycolide) sintered microsphere scaffolds for bone tissue engineering. Biotechnol Bioeng 2007;98:1094–102.
[31] De Bari C, Dell'Accio F, Karystinou A, Guillot PV, Fisk NM, Jones EA, et al. Biomarker-based mathematical model to predict bone-forming potency of human synovial and periosteal mesenchymal stem cells. Arthritis Rheum 2008;58:240–50.
[32] Wang D-A, Williams CG, Yang F, Cher N, Lee H, Elisseeff JH. Bioresponsive phosphoester hydrogels for bone tissue engineering. Tissue Eng 2005;11:201–13.
[33] Meyer U, Wiesmann HP. Bone and cartilage engineering. Heidelberg: Springer; 2006. p. 7–43.
[34] Harada SI, Rodan GA. Control of osteoblast function and regulation of bone mass. Nature 2003;423:349–55.
[35] Fleisch H. Bisphosphonates: mechanisms of action. Endocr Rev 1998;19(1):80–100.
[36] Russell RG, Rogers MJ. Bisphosphonates: from the laboratory to the clinic and back again. Bone 1999;25:97–106.
[37] Rodan GA. Mechanism of action of bisphosphonates. Annu Rev Pharmacol Toxicol 1998;38:375–88.
[38] Rodan GA, Martin TJ. Therapeutic approaches to bone diseases. Science 2000;289:1508–14.
[39] Tsagozis P, Eriksson F, Pisa P. Zoledronic acid modulates antitumoral responses of prostate cancer-tumor associated macrophages. Cancer Immunol Immunother 2008;57:1451–9.
[40] Pandey R, Quinn JMW, Sabokbar A, Athanasou NA. Bisphosphonate inhibition of bone resorption induced by particulate biomaterial-associated macrophages. Acta Orthop Scand 1996;67:221–8.
[41] Mundy G, Garrett R, Harris S, Chan J, Chen D, Rossini G, et al. Stimulation of bone formation in vitro and in rodents by statins. Science 1999;286:1946–9.
[42] Nieto A, Balas F, Colilla M, Manzano M, Vallet-Regí M. Functionalization degree of SBA-15 as key factor to modulate sodium alendronate dosage. Microporous Mesoporous Mater 2008;116:4–13.
[43] Lao L, Tan H, Wang Y, Gao C. Chitosan modified poly(L-lactide) microspheres as cell microcarriers for cartilage tissue engineering. Colloid Surf B 2008;66:218–25.
[44] Wang C, Gong Y, Lin Y, Shen J, Wang D-A. A novel gellan gel-based microcarrier for anchorage-dependent cell delivery. Acta Biomater 2008;4:1226–34.
[45] Wang C, Gong Y, Zhong Y, Yao Y, Su K, Wang D-A. The control of anchorage-dependent cell behavior within a hydrogel/microcarrier system in an osteogenic model. Biomaterials 2009;30:2259–69.
[46] Park K, Park JS, Woo DG, Yang HN, Chung H-M, Park K-H. The use of chondrogenic differentiation drugs to induce stem cell differentiation using double bead microsphere structure. Biomaterials 2008;29:2490–500.
[47] Wang D-A, Williams CG, Yang F, Elisseeff JH. Enhancing the tissue–biomaterial interface: tissue-initiated integration of biomaterials. Adv Funct Mater 2004;14:1152–9.
[48] Wang D-A, Varghese S, Sharma B, Strehin I, Fermanian S, Gorham J, et al. Multifunctional chondroitin sulphate for cartilage tissue–biomaterial integration. Nat Mater 2007;6:385–92.
[49] Li Q, Wang D-A, Elisseeff JH. Heterogeneous-phase reaction of glycidyl methacrylate and chondroitin sulfate: mechanism of ring-opening-transesterification competition. Macromolecules 2003;36:2556–62.
[50] Borden M, Attawia M, Khan Y, Laurencin CT. Tissue engineering microsphere-based matrices for bone repair: design and evaluation. Biomaterials 2002;23:551–9.